Science Translational Medicine
AAAS

stm.sciencemag.org/cgi/content/full/11/508/eaaw8828/DC1

Supplementary Materials for

Overcoming adaptive therapy resistance in AML by targeting immune response pathways

Katelyn Melgar, Morgan M. Walker, LaQuita M. Jones, Lyndsey C. Bolanos, Kathleen Hueneman, Mark Wunderlich, Jiang-Kang Jiang, Kelli M. Wilson, Xiaohu Zhang, Patrick Sutter, Amy Wang, Xin Xu, Kwangmin Choi, Gregory Tawa, Donald Lorimer, Jan Abendroth, Eric O'Brien, Scott B. Hoyt, Ellin Berman, Christopher A. Famulare, James C. Mulloy, Ross L. Levine, John P. Perentesis, Craig J. Thomas*, Daniel T. Starczynowski*

*Corresponding author. Email: craigt@mail.nih.gov (C.J.T.); daniel.starczynowski@cchmc.org (D.T.S.)

Published 4 September 2019, *Sci. Transl. Med.* **11**, eaaw8828 (2019)
DOI: 10.1126/scitranslmed.aaw8828

The PDF file includes:

Other Supplementary Material for this manuscript includes the following:

(available at stm.sciencemag.org/cgi/content/full/11/508/eaaw8828/DC1)

Table S3. Gene expression analysis of FLT3-ITD AML treated with FLT3i.
Table S4. AML patients evaluated with gilteritinib.
Table S5. Reaction Biology profile of NCGC1481.
Table S6. KiNativ profile of NCGC1481 in MV4;11 lysate.
Table S7. Characteristics of patients with AML.
Table S8. Peptide phosphorylation in the PamChip serine-threonine in-cell kinase array with NCGC1481 treatment.
Table S9. Gene expression analysis of FLT3-ITD AML treated with NCGC1481.
Data file S2 (Microsoft Excel format). Original data.

Supplementary Materials
Materials and Methods

Reagents

IRAK1/4 inhibitor (Amgen Inc.) was purchased from Sigma-Aldrich (Cat#I5409). Quizartinib was purchased from Selleckchem (Cat#S1526). IKK7 was purchased from Selleckchem (Cat#S2882). Gilteritinib was purchased from Chemietik (Cat#CT-GILT). ODN-INH-18 was purchased from InvivoGen (Cat#tlrl-inh18). PF06650833 (PF066) was purchased from Sigma-Aldrich (PZ0327-5MG). The TLR9 antagonist, ODN-INH-18, was purchased from InvivoGen (Cat#tlrl-inh18).

DNA sequencing

To isolate whole genomic DNA, cell pellets were resuspended in NaOH (50 mM) and incubated at 95° C for 1 hour. Samples were centrifuged, and the supernatant pH was neutralized with Tris-HCl (1 M). The FLT3 kinase domain was amplified by PCR from whole genomic DNA using GeneAmp Fast PCR Mastermix (Applied Biosystems, Cat#28796). The PCR product was extracted using QIAquick Gel Extraction Kit (Qiagen, Cat#28706). For amplification and bidirectional sequencing of the F691 locus, the following primers were used: Forward - 5'-GAGAGGCACTCATGTCAGAACTCA-3', reverse - 5'-AGTCCTCCTCTTCTTCCAGCCTTT-3' (*21*). For the D835 locus, the following primers were used: Forward - 5'-TGTGTTCACAGAGACCTGGC-3', reverse - 5'-TTTACAGGCAGACGGGCATT-3'. For the NRAS G12/13 locus, the following primers were used: Forward – 5'-ATTAATCCGGTGTTTTTGCGTTCT-3', reverse – 5'-CATCTCTGAATCCTTTATCTCCAT-3' (*93*).

Immunoblotting

Protein lysates were made by lysing cells in cold RIPA lysis buffer (50 mM Tris-HCl, 150 mM NaCl, 1 mM ethylenediaminetetraacetic acid (EDTA), 1% Triton X-100, and 0.1% sodium dodecyl sulfate (SDS)) in the presence of sodium orthovanadate, phenylmethylsulfonyl fluoride (PMSF), and protease and phosphatase inhibitors. Protein concentration was quantified using bicinchoninic acid (BCA) assay (Pierce, Cat#23225). Protein lysates were separated by SDS-polyacrylamide gel electrophoresis (BIO-RAD), transferred to nitrocellulose membranes (BIO-RAD, Cat#1620112), and immunoblotted. The following antibodies were used for western blot analysis: GAPDH (Cell Signaling, Cat#D16H11, 1:1000 milk), FLT3 (Cell Signaling, Cat#3462, 1:500 BSA), phospho-FLT3 (Tyr591) (Cell Signaling, Cat#3461, 1:500 BSA), IRAK4 (Cell Signaling, Cat#4363, 1:1000 BSA), phospho-IRAK4 (Thr345/Ser346) (Cell Signaling, Cat#11927, 1:500 BSA), IRAK1 (H-273) (Santa Cruz, Cat#sc-7883, 1:1000 milk), phospho-IRAK1 (T209) (Assay Biotech, Cat#A1074, 1:500 BSA), JNK2 (Cell Signaling, Cat#9258, 1:1000 BSA), phospho-SAPK/JNK (Thr183/Tyr185) (Cell Signaling, Cat#4668, 1:500 BSA), p38 MAPK (Cell Signaling, Cat#9212, 1:1000 BSA), phospho-p38 MAPK (Thr180/Tyr182) (Cell Signaling, Cat#4631, 1:500 BSA), STAT5 (Cell Signaling, Cat#9363, 1:1000 BSA), phospho-STAT5 (Cell Signaling, Cat#9351, 1:1000 BSA), phospho-SRC Family (Tyr416) (Cell Signaling, Cat#2101, 1:1000 BSA), SRC (Cell Signaling, Cat#2108, 1:1000 BSA), TLR9 (Cell Signaling, Cat#2254, 1:1000 BSA), peroxidase-conjugated AffiniPure goat anti-rabbit IgG (Jackson ImmunoResearch Laboratories, Inc., Cat#111-035-003, 1:10000 milk). Blots were visualized using ECL Western Blotting Substrate (Pierce, Cat#32106) and imaged on

autoradiography film (HyBlot CL) or BIO-RAD ChemiDoc Touch Imaging system.

In vitro cellular studies

For colony formation, cells were suspended at 1000 cells/ml in methylcellulose (MethylCult H4434 Classic, Cat#04434). Colonies were counted 7-10 days after plating. AnnexinV viability staining was carried out according to manufacturer's instructions (AnnexinV Binding Buffer: Invitrogen, Cat#00-0055-56; AnnexinV-APC conjugated antibody: 1:100, eBioscience, Cat#88-8007). Analysis was performed using BD FACSCanto flow cytometer with Diva software. Trypan Blue (Invitrogen, Cat#T10282) exclusion was done using an automated cell counter (BioRad TC10). CellTiter Glo Luminescent Viability Assay (Promega, Cat#G7572) was performed according to manufacturer protocol. Analysis was performed using GloMax 96 microplate Luminometer (Promega) with GloMax Software.

NF-κB activation reporter

THP1-Blue NF-κB SEAP reporter cells were grown in a 96-well plate in triplicate with the indicated inhibitor for 24 hours. In a new 96-well plate, 20 µl of cell supernatant was added to 180 µl of warmed QuantiBlue Reagent (Invivogen, Cat#rep-qbs2) and incubated at 37 °C for 30 minutes. Absorbance was read at 630 nm.

Synergy matrix analysis

The compound synergy analysis and calculations have been previously described (*94*). Briefly, MA9 FLT3-ITD cells were treated with 10 doses of quizartinib and 10 doses of IRAK-Inh in a 10 x 10 combination matrix for 48 hours. Viability was assessed using CellTiter-Glo, and then a delta Bliss score was calculated for each drug combination using the Bliss independence model.

IRAK4 crystallography

We expressed $IRAK4_{160-460}$ with the addition of a TEV-cleavable octa-histidine tag at the N-terminus in Sf9 insect cells. The protein was purified by nickel affinity chromatography, then the histidine tag was removed by cleavage with TEV protease and the protein was subjected to a second nickel affinity chromatography step. The flow-through from the second Ni affinity step was further purified by size-exclusion chromatography in 20 mM Tris-HCl, pH 8.0, 1 mM DTT. The protein was concentrated to 9.5 mg/ml for crystallization. Crystals were grown in the MCSG1 screen (Microlytics), condition E10: 0.2 M ammonium tartrate dibasic, 20% (*w/v*) PEG3350 with 1 mM NCGC00371481 and cryopreserved in 20% (*v/v*) ethylene glycol with 1 mM NCGC00371481. The crystals grew in 13 days at 14^{o}C. The IRAK4-NCGC00371481 structure crystallized in the C*2* space group, with unit cell dimensions *a*=138.29 Å, *b*=141.91 Å, *c*= 87.89 Å, β = 126.22^{o}. We collected X-ray data using a Rigaku SuperBright FR-E+ X-ray generator with Osmic VariMax HF optics and a Saturn 944+ CCD detector.

Chemical characterization

NCGC1481: 6-(7-methoxy-6-(1-methyl-1H-pyrazol-4-yl)imidazo[1,2-a]pyridin-3-yl)-N-(pyrrolidin-3-yl)pyridin-2-amine: ^{1}H NMR (400 MHz, DMSO-d_6) δ 9.88 (s, 1H), 8.90 (br.s, 1H), 8.78 (br.s, 1H), 8.44 (s, 1H), 8.22 (s, 1H), 7.90 (d, *J* = 0.8 Hz, 1H), 7.62 (dd, *J* = 8.4, 7.4 Hz, 1H), 7.36 (s, 1H), 7.22 – 7.17 (m, 2H), 6.56 (d, *J* = 8.3 Hz, 1H), 4.59 – 4.55 (m, 1H), 4.08 (s, 3H), 3.91 (s, 3H), 3.25 – 3.17 (m, 2H), 2.20 – 2.11 (m, 1H), 2.08 – 1.99 (m, 1H). HRMS: *m/z* $(M+H)^{+}$ = 389.1964 (Calculated for $C_{21}H_{23}N_7O$ = 389.1964).

Quantitative analysis of quizartinib and NCGC1481 in mouse plasma

Ultra-performance liquid chromatography-tandem mass spectrometry (UPLC-MS/MS) methods were developed to determine quizartinib and NCGC1481 concentrations in mouse plasma samples. Mass spectrometric analysis was performed on a Waters Xevo TQ-S triple quadrupole instrument using electrospray ionization in positive mode with the selected reaction monitoring. The separation of test compounds from endogenous components was performed on an Acquity BEH C18 column (50 x 2.1 mm, 1.7 µm) using a Waters Acquity UPLC system with 0.6 ml/min flow rate and gradient elution. The mobile phases were 0.1% formic acid in water and 0.1% formic acid in acetonitrile. The calibration standards and quality control samples were prepared in untreated mouse plasma. Aliquots of 10 µl plasma samples were mixed with 200 µl internal standard in acetonitrile to precipitate proteins in a 96-well plate. 0.5 µl supernatant was injected for the UPLC-MS/MS analysis. Data were analyzed using MassLynx V4.1 (Waters Corp.). Adult male NRGS mice (n = 3/sampling time point) were obtained from Jackson Laboratory. All experimental procedures were approved by the Animal Care and Use Committee (ACUC) of the NIH Division of Veterinary Resources (DVR). A single dose of 30 mg/kg was administered IP. Dosing solutions were freshly prepared on the day of administration in saline. The blood samples (~ 80 µl) were collected via tail vein in K2EDTA tubes at 0.083, 0.25, 0.5, 1, 2, 4, 7, and 24 hours after drug administration, and plasma (~ 30 µl) was harvested after centrifugation at 3000 rpm for 10 min. All plasma samples were stored at -80°C until analysis. The pharmacokinetic parameters were calculated using the non-compartmental approach (Model 200) of the pharmacokinetic software Phoenix WinNonlin, version 6.2 (Certara). The area under the plasma concentration versus time curve (AUC) was calculated using the linear trapezoidal method. The slope of the apparent terminal phase was estimated by log linear regression using at least 3 data points, and the terminal rate constant (λ) was derived from the slope. $AUC_{0-\infty}$ was estimated as the sum of the AUC_{0-t} (where t is the time of the last measurable concentration) and Ct/λ. The apparent terminal half-life ($t_{½}$) was calculated as $0.693/\lambda$.

2-Dimentional (2D) interactions for NCGC1481 bound to IRAK4 and FLT3

The 2D interaction diagrams were generated using MOE (*95*).The crystal structure coordinates of the NCGC1481-IRAK4 complex and the NCGC1481-FLT3 complex (6MOM.pdb, 6IL3.pdb respectively) where loaded into MOE. The diagrams were then drawn by running the “Ligand interactions” module. The ligand interactions module proceeds by ascertaining the interactions between the ligand and the protein (*96*), positioning the relevant protein residues around the ligand in a 2D format, drawing the ligand-protein interactions and then estimating a proximity contour around the ligand that roughly defines the interface between ligand and protein or solvent.

Alignment of IRAK4 and FLT3 sequences

The sequence alignment and annotation was done using MOE. MOE uses an alignment algorithm based on a modified version of the alignment methodology as previously described (*97*).

Kinome screens

Dissociation constants (Kd) were measured at DiscoverX using the KINOME*scan* Profiling Service. Kinase inhibition (IC50s) was measured at Reaction Biology using the Kinase Assay service.

Supplementary Figures

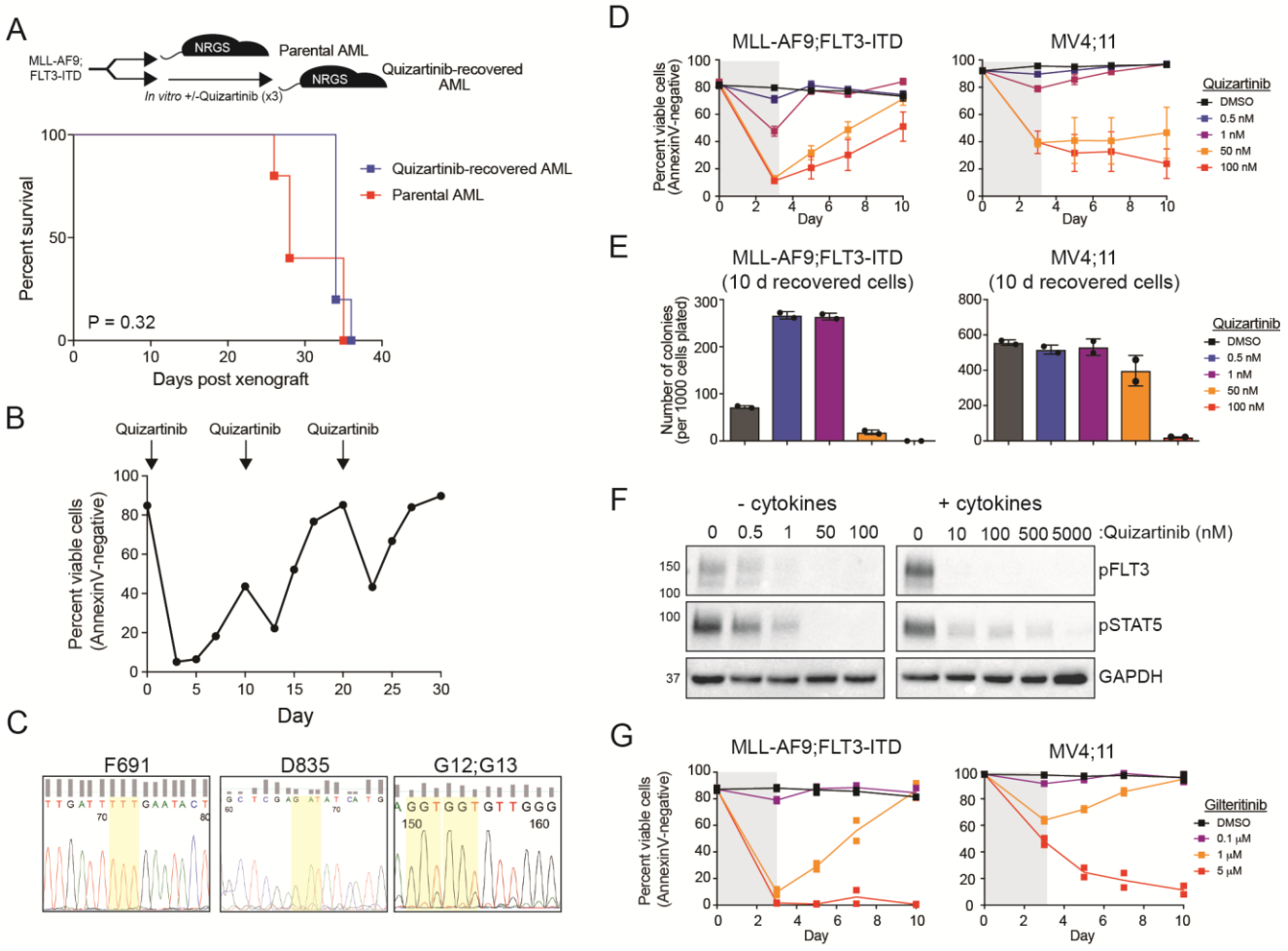

Fig. S1. FLT3+ AML develop adaptive resistance to FLT3i. (A) Quizartinib-recovered MLL-AF9;FLT3-ITD cells (from panel B) or parental MLL-AF9;FLT3-ITD cells (n = 5 mice per group) were transplanted into NRGS mice (n = 5 mice per group). Disease free survival shown via Kaplan-Meier curve. P = 0.32, Mantel-Cox test. **(B)** MLL-AF9;FLT3-ITD cells were cultured with quizartinib (5 μM) for 3 days and re-plated in fresh medium. After 7 days, cells were treated with quizartinib (5 μM) for 3 days and re-plated in fresh medium. After 7 days, cells were treated for a third time with quizartinib (5 μM) for 3 days and re-plated in fresh medium. AnnexinV staining was used to measure cell viability. **(C)** Genomic DNA from quizartinib-recovered MLL-AF9;FLT3-ITD cells (from panel B) was sequenced at the FLT3 F691 and D835 loci, and NRAS G12 and G13 loci. **(D)** MLL-AF9;FLT3-ITD cells or MV4;11 cells were cultured in standard medium without cytokines and then treated with quizartinib for 3 days, re-plated in fresh medium, and then cell viability was measured by AnnexinV staining. **(E)** After 10 days in liquid culture (from panel D), the remaining viable cells were plated in methylcellulose and colony formation was determined after 7 days (n = 2 per condition). Values are expressed as means +/- SD from 2 biological replicates. **(F)** Immunoblotting of MLL-AF9;FLT3-ITD cells grown with and without IL-3, IL-6, SCF, TPO, and FL (10 ng/mL) and treated with quizartinib for 24 hours. **(G)** MLL-AF9;FLT3-ITD cells or MV4;11 cells were cultured with gilteritinib for 3 days, re-plated in fresh medium, and then cell viability was measured by AnnexinV staining. Individual data points are shown along with the mean from 2 biological replicates.

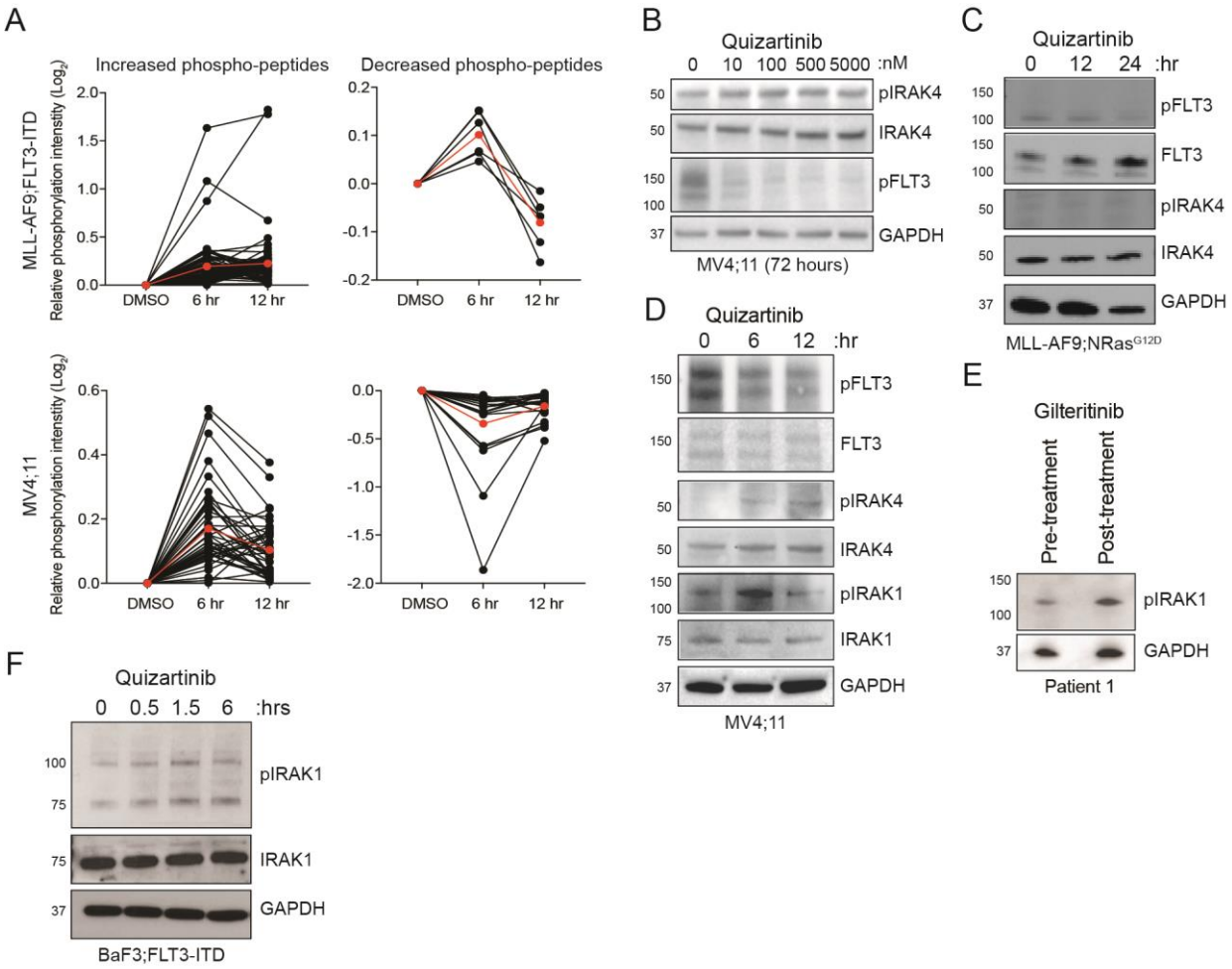

Fig. S2. Adaptively resistant FLT3+ AML exhibit increased IRAK1/4 activation. (A) MLL-AF9;FLT3-ITD or MV4-11 cells treated with quizartinib showed two distinct patterns of peptide phosphorylation in the STK PamChip. Red line indicates the average phosphorylation within each group. **(B)** Immunoblotting of pIRAK4 and pFLT3 from MV4;11 cells treated with quizartinib for 72 hours. **(C)** Immunoblotting of MLL-AF9;NRAS-G12D cells treated with quizartinib (50 nM). **(D)** Immunoblotting of the indicated proteins in MV4;11 cells treated with quizartinib (0.3 nM) for the indicated times. **(E)** Immunoblotting of pIRAK1 and GAPDH from the peripheral blood of a FLT3-ITD AML patient treated with gilteritinib for 27 days. **(F)** Immunoblotting of pIRAK1 and IRAK1 in BaF3 cells expressing FLT3-ITD treated with quizartinib (50 nM) for the indicated times.

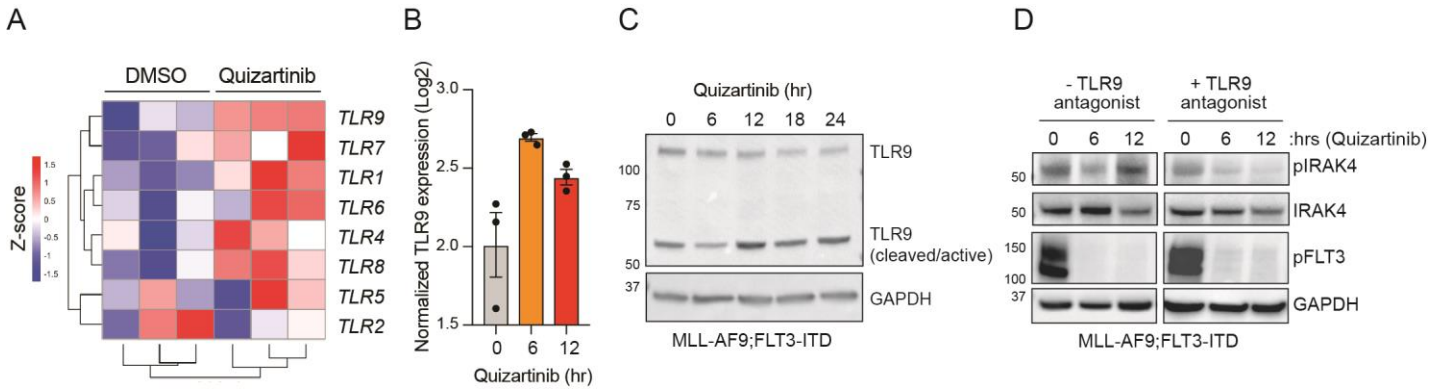

Fig. S3. Quizartinib induces TLR9-mediated activation of IRAK4. (A) RNA expression of the indicated TLRs in MLL-AF9;FLT3-ITD cells after 6 hours of treatment with quizartinib. **(B)** RNA expression of TLR9 in MLL-AF9;FLT3-ITD cells after treatment with 10 nM quizartinib for 6 hours. **(C)** Immunoblotting of TLR9 in MLL-AF9;FLT3-ITD cells after treatment with 10 nM quizartinib for the indicated time points. The full-length and cleaved forms of TLR9 are shown. **(D)** Immunoblotting of the indicated proteins in MLL-AF9;FLT3-ITD cells after treatment with 10 nM quizartinib and 30 nM of the TLR9 antagonist (ODN-INH-18) for the indicated time points.

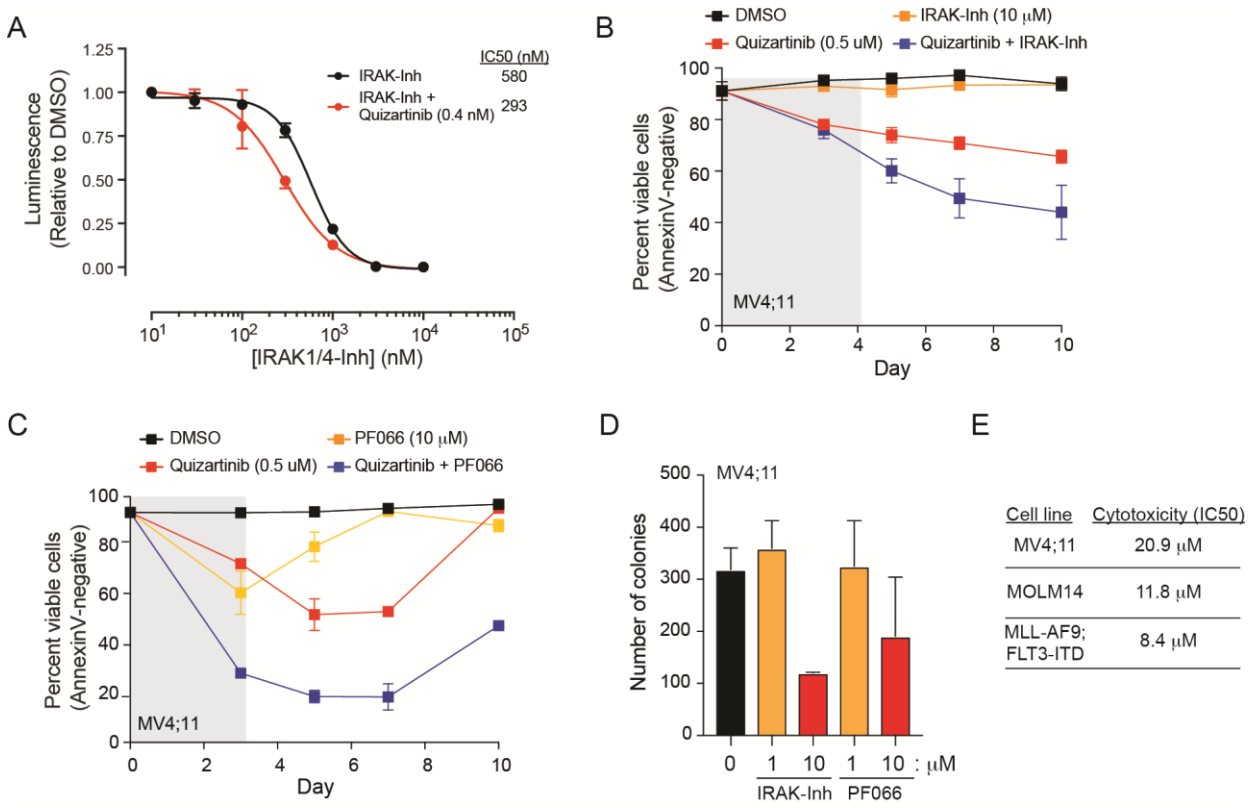

Fig. S4. Inhibition of IRAK1/4 sensitizes FLT3+ AML to quizartinib. (A) CellTiter-Glo was used to measure metabolic activity of MLL-AF9;FLT3-ITD cells treated with IRAK-Inh alone, or with IRAK-Inh and quizartinib (0.4 nM). **(B)** MV4;11 cells were treated with DMSO, quizartinib (0.5 μM), IRAK-Inh (10 μM), or Quizartinib and IRAK-Inh for 3 days, and then viability was evaluated every 2 days by AnnexinV staining. **(C)** MV4;11 cells were treated with DMSO, quizartinib (0.5 μM), PF066 (IRAK4-Inh; 10 μM), or quizartinib and PF066 for 3 days, and then viability was evaluated every 2 days by AnnexinV staining. **(D)** MV4;11 cells were treated with IRAK-Inh or PF066 in methylcellulose and then colonies were evaluated after 10 days. **(E)** CellTiter-Glo was used to measure metabolic activity of the indicated cell lines treated with ten doses of the IRAK4 inhibitor PF066.

A

NCGC1481	
MW	389.46
tPSA	76.85
CLogP	2.19

B

Assay	Result
Microsomal $t_{1/2}$ (r/m/h, min)	>120 / 13 / >120
Solublity @ pH 7.4 (μM)	>58
CYP3A4/2C9/2D6 IC50 (μM)	4.8 / 9.4 / 0.09
hERG/Nav1.5/Cav2.2 (% inh. @ 10μM)	1% / 0% / 11%

C

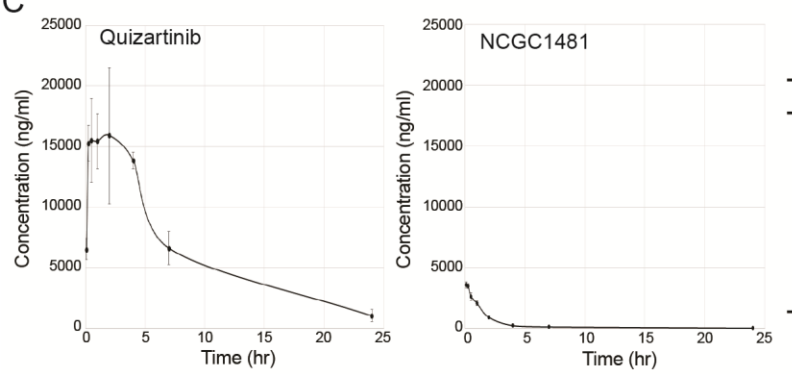

Parameter	Units	Quizartinib	NCGC1481
Dose	mg/kg	30	30
AUClast	hr*ng/ml	155000	6750
SE AUClast	hr*ng/ml	9700	226
AUCINF/D	hr*kg*ng/ml/mg	5440	227
T1/2	hr	5.7	4.2
Tmax	hr	2	0.083
Cmax	ng/ml	15900	3570
Cmax/D	kg*ng/ml/mg	530	119

D

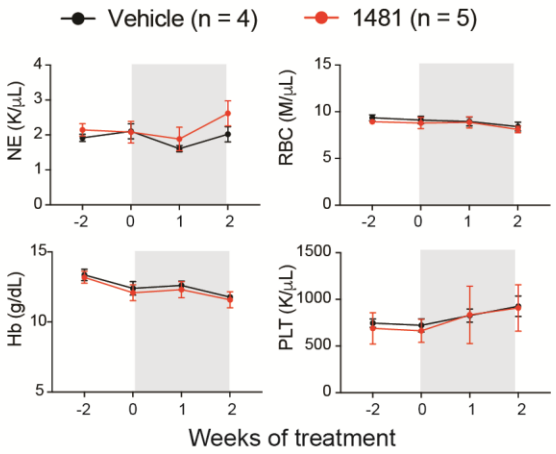

E

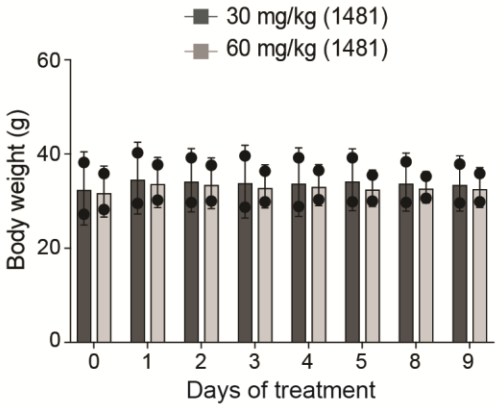

Fig. S5. NCGC1481 exhibits promising physicochemical and in vivo pharmacokinetic properties. (A) Molecular weight (MW, g/mol), topological polar surface area (tPSA, angstroms squared), and logarithm of partition coefficient (cLogP) for NCGC1418. **(B)** Microsomal stability (rat, mouse, human), aqueous solubility, CYP inhibition (3A4, 2C9, 2D6), ion channel inhibition (hERG, Nav1.5, Cav2.2) for NCGC1481. All assays measured at a 10 μM concentration of NCGC1481. **(C)** Plasma concentrations of quizartinib and NCGC1481 in mice after intraperitoneal injection measured at the indicated time points over 24 hours. Three mice per time point were evaluated. AUC, area under the plasma concentration over time curve; AUC_{last}, AUC calculated to the last measurable concentration; SE AUC_{last}, standard error for AUC_{last}; AUC_{INF}/D, AUC extrapolated to infinity and divided by the dose; $T_{1/2}$, terminal half-life; C_{max}, maximum concentration; C_{max}/D, C_{max} divided by the dose; Tmax, time to reach Cmax. **(D)** Blood counts performed at the indicated time points on mice treated daily with 30 mg/kg IP of NCGC1481. **(E)** Body weight measurements of NRGS mice treated with 30 or 60 mg/kg of NCGC1481 for the indicated number of days. Values are expressed as means +/- SD from 2 biological replicates.

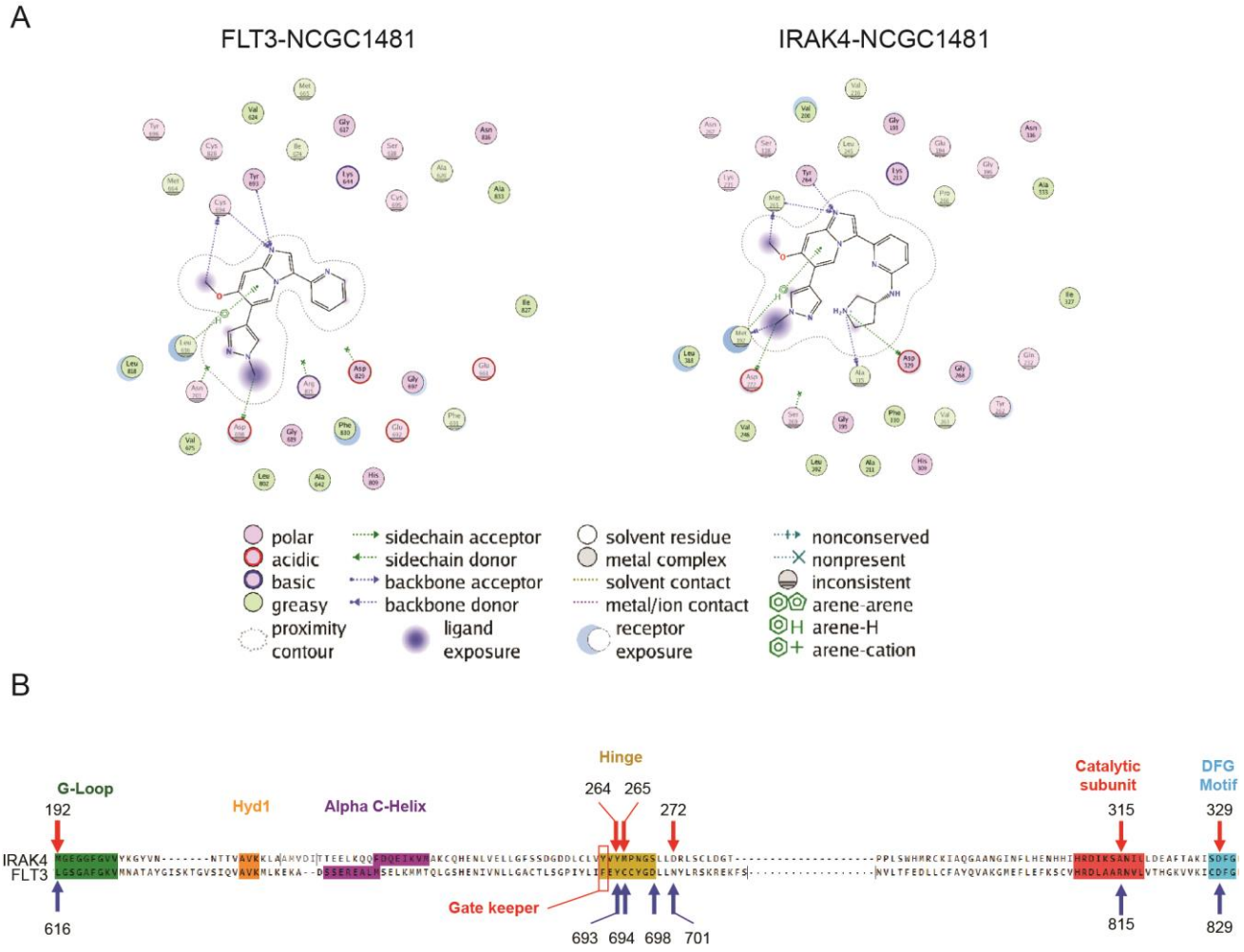

Fig. S6. 2D interaction diagrams for NCGC1481 bound to FLT3 and IRAK4. (A) The crystal structure coordinates of the NCGC1481-FLT3 complex (left) and the NCGC1481-IRAK4 complex (right) are shown as a 2-dimentional interaction diagram. The elements of the 2-dimentional image are illustrated in the legend below. **(B)** Alignment of IRAK4 and FLT3 amino acid sequences and associated sequence annotation.

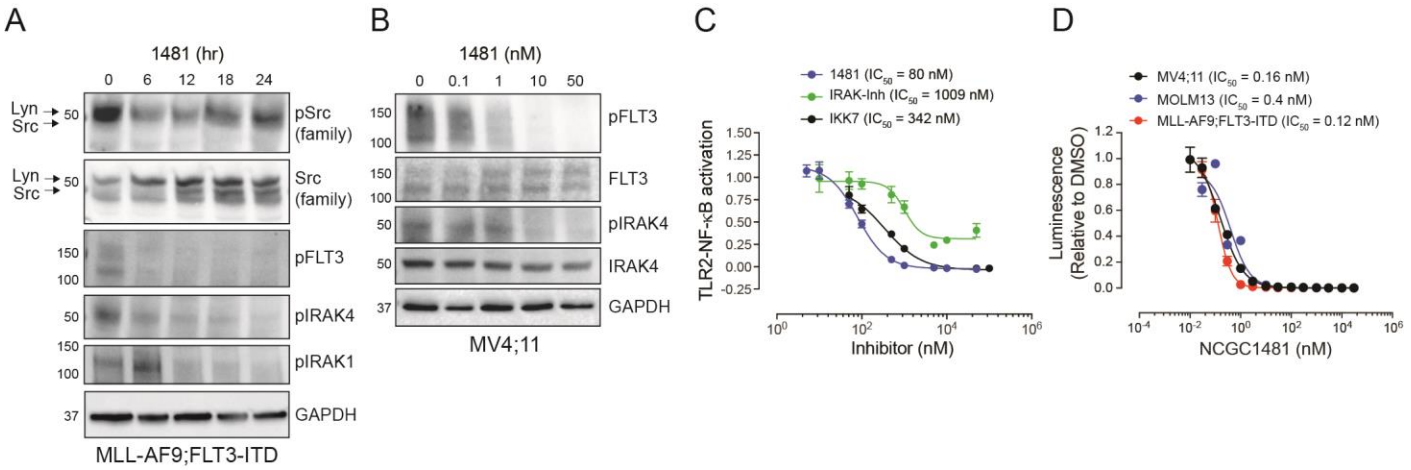

Fig. S7. NCGC1481 inhibits compensatory IRAK1/4 activation and adaptive resistance of FLT3-ITD AML. (A) Immunoblotting of MLL-AF9;FLT3-ITD cells treated with 10 nM NCGC1481 for the indicated hours. **(B)** Immunoblotting of MV4;11 cells treated with NCGC1481 for 24 hours. **(C)** Relative NF-κB activity in Pam3CSK4-stimulated THP1-NF-κB reporter cells treated with NCGC1481, IKK7, or IRAK-Inh for 24 hours was measured via QuantiBlue Reagent. Values are expressed as means +/- SEM from 3 biological replicate samples. **(D)** Proliferation of MLL-AF9;FLT3-ITD, MV4;11, and MOLM13 cells treated with NCGC1481 for 72 hours as measured by CellTiter-Glo. Values are expressed as means +/- SEM from 3 biological replicate samples.

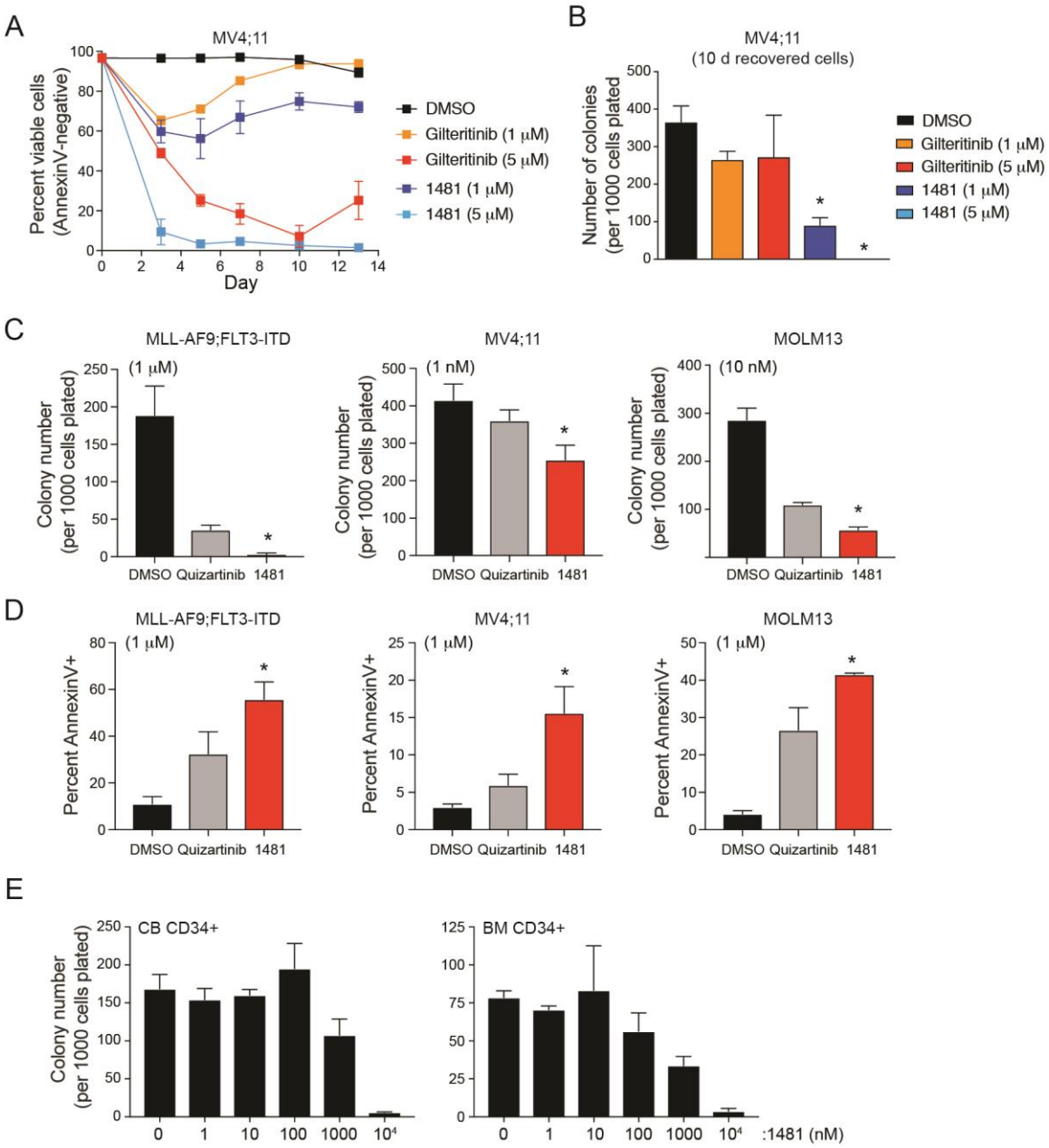

Fig. S8. NCGC1481 prevents adaptive resistance of FLT3-ITD AML cells in vitro and has minimal effects on normal hematopoietic cells. (A) MV4;11 cells were cultured with gilteritinib or NCGC1481 for 3 days, re-plated in fresh medium, and then cell viability was measured by AnnexinV staining. Values are expressed as means +/- SEM from 3 biological replicates. **(B)** After 10 days in liquid culture (from panel A), the remaining viable cells were plated in methylcellulose and colony formation was determined after 7 days (n = 4 per condition). *, $P < 0.05$ (unpaired, two-tailed t-test). **(C)** MLL-AF9;FLT3-ITD (n = 6), MV4;11 (n = 3), and MOLM13 (n = 3) cells were plated in methylcellulose and treated with DMSO, quizartinib, or NCGC1481 at the indicated concentrations. Colony formation was determined after 7 days (n = 3 per condition). *, $P < 0.05$ (unpaired, two-tailed t-test). **(D)** MLL-AF9;FLT-ITD (n = 4), MV4;11 (n = 2), and MOLM13 (n = 2) cells were treated with DMSO, quizartinib, or 1481 for 3 days and cell death was measured using AnnexinV. *, $P < 0.05$ (unpaired, two-tailed t-test). **(E)** Normal human CD34+ cord blood cells or normal human CD34+ bone marrow (BM) cells were plated in methylcellulose with the indicated concentrations of NCGC1481. Colony formation was determined after 12 days (n = 3 per condition).

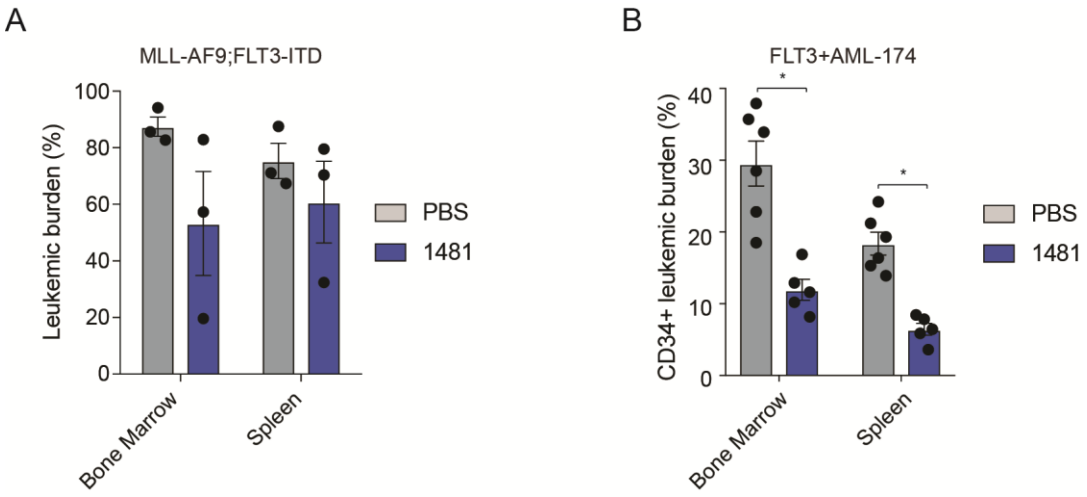

Fig. S9. NCGC1481 reduces the leukemic burden of FLT3-ITD AML. (A) Leukemic burden (%GFP+) in bone marrow (BM) and spleen at time of sacrifice in NRGS mice transplanted with MLL-AF9;FLT3-ITD cells and treated with PBS or 1481 (30 mg/kg) IP daily. **(B)** Leukemic burden (%CD34+) in BM and spleen at time of sacrifice in NSGS mice transplanted with FLT3+AML-174 and treated with PBS or 1481 (30 mg/kg) IP daily.*, $P < 0.05$ (unpaired, two-tailed t-test).

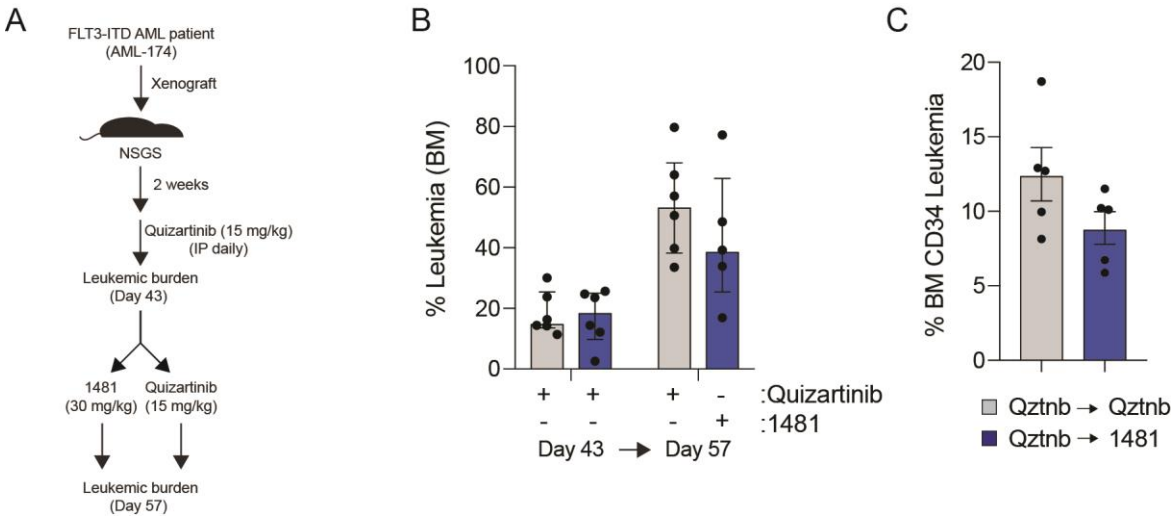

Fig. S10. NCGC1481 reduces the leukemic burden of FLT3-ITD AML after quizartinib treatment. (A) Overview of experimental design of xenograft studies using patient-derived FLT3-ITD AML cells (AML-174). AML cells were i.v. injected into NSGS mice. Two weeks post-transplant, mice were treated with quizartinib (15 mg/kg) IP daily. On day 43 (after leukemic burden has been established), half of the mice were switched to daily NCGC1481 (30 mg/kg) and the other half remained on quizartinib (n = 5 mice per group). **(B)** Leukemic burden (% human CD45+) in the bone marrow (BM) was determined on days 43 and 57. **(C)** Leukemic stem cell burden (% human CD34+) in the BM was determined on day 57. P = 0.12 (unpaired, two-tailed t-test).